Variability and trends in stratospheric NO2 in Antarctic summer, and implications for stratospheric NOy

Atmos. Chem. Phys., 9, 3601–3612, 2009
www.atmos-chem-phys.net/9/3601/2009/

Atmospheric Chemistry and Physics

Variability and trends in stratospheric NO_2 in Antarctic summer, and implications for stratospheric NO_y

P. A. Cook and H. K. Roscoe

British Antarctic Survey, Madingley Rd, Cambridge CB3 0ET, UK

Received: 1 September 2008 – Published in Atmos. Chem. Phys. Discuss.: 12 January 2009
Revised: 23 March 2009 – Accepted: 14 May 2009 – Published: 4 June 2009

Abstract. NO_2 measurements during 1990–2007, obtained from a zenith-sky spectrometer in the Antarctic, are analysed to determine the long-term changes in NO_2. An atmospheric photochemical box model and a radiative transfer model are used to improve the accuracy of determination of the vertical columns from the slant column measurements, and to deduce the amount of NO_y from NO_2. We find that the NO_2 and NO_y columns in midsummer have large inter-annual variability superimposed on a broad maximum in 2000, with little or no overall trend over the full time period. These changes are robust to a variety of alternative settings when determining vertical columns from slant columns or determining NO_y from NO_2. They may signify similar changes in speed of the Brewer-Dobson circulation but with opposite sign, i.e. a broad minimum around 2000. Multiple regressions show significant correlation with solar and quasi-biennial-oscillation indices, and weak correlation with El Nino, but no significant overall trend, corresponding to an increase in Brewer-Dobson circulation of 1.4±3.5%/decade. There remains an unexplained cycle of amplitude and period at least 15% and 17 years, with minimum speed in about 2000.

1 Introduction

The circulation whereby air enters the stratosphere in the tropics, continues toward the winter pole, and returns to the troposphere via tropopause folds at mid-latitudes, is known as the Brewer-Dobson circulation after its discoverers (Brewer, 1949; Dobson, 1956). It is now known to be driven by the breaking of planetary-scale Rossby waves and of gravity waves, against the mean zonal winds, in the stratosphere and mesosphere. This provides the necessary friction-like force to allow poleward flow on a rotating earth in an otherwise almost frictionless fluid.

Changes in the speed of the Brewer-Dobson circulation will affect the stratospheric concentrations of longer-lived trace gases whose sources are in the troposphere (e.g. CFCs, CH_4, N_2O), as well as of their eventual stratospheric products (e.g. reactive chlorine gases, H_2O, reactive nitrogen gases). Changes in its speed will also affect the tropospheric concentrations of trace gases with large sources in the stratosphere (e.g. ozone). Because these gases are important to atmospheric climate and chemistry, it is important to know what changes have occurred to the Brewer-Dobson circulation in the past and will occur in future. A slowing of the circulation would allow more time in the stratosphere for the reactions of N_2O to reactive nitrogen. Hence, if tropospheric N_2O and other factors remained constant, an upwards trend in the vertical column of reactive nitrogen gases in the stratosphere would indicate a slowing of the circulation.

Tropospheric N_2O is increasing by about 2.5%/decade (WMO 2007), but measured slant columns of NO_2 from Lauder, New Zealand (45° S) between 1980 and 1998 show an upwards trend of about 5%/decade (Liley et al., 2000), demonstrating that further processes are involved, several of which were discussed and evaluated by McLinden et al. (2001).

The speed of the Brewer-Dobson circulation will change as planetary and gravity wave intensities are changed, for example due to increased greenhouse gases or to volcanic aerosol. Most climate models suggest that the speed of the Brewer-Dobson circulation should increase as greenhouse gases increase (see Sect. 6). But changes in wave amplitudes are difficult to accurately diagnose from meteorological analyses, particularly for gravity waves, most of which are below the grid scale of current analysis models.

In this paper, we assess trends in stratospheric reactive nitrogen in the hope that it can be used to diagnose changes in the Brewer-Dobson circulation. We examine trends in NO_2

Correspondence to: H. K. Roscoe
(hkro@bas.ac.uk)

Published by Copernicus Publications on behalf of the European Geosciences Union.

in the Antarctic summer, where it is easy to calculate the implied total reactive nitrogen because of the almost complete absence of N_2O_5, an otherwise important component of the reactive nitrogen family. N_2O_5 also hydrolyses on aerosol, thereby converting NO_2 to HNO_3, so its comparative absence in the Antarctic summer means that NO_2 is little affected by stratospheric aerosol.

We use NO_2 data from a zenith-sky spectrometer that was set up at Faraday in the Antarctic (65.25° S, 64.27° W) between 1990 and 1995, and has now been at the nearby site of Rothera (67.57° S, 68.13° W) since 1996, providing almost continuous measurements of Antarctic NO_2 since before the eruption of Mt. Pinatubo (Roscoe et al., 2001; Roscoe, 2004).

2 Apparatus and spectral analysis

Zenith-sky spectrometers, which continuously look at the zenith and record the spectra of scattered sunlight to obtain slant columns of NO_2 and ozone, have been used in the Antarctic for many years (Mount et al., 1987; Pommereau and Goutail, 1988a and 1988b). Our instrument was of the SAOZ design the latter describe. Briefly, a small spectrometer with resolution about 1 nm is housed in an outdoor box, observing light from 300 to 600 nm. An ambient-temperature array detector observes all the spectrum at once, so that clouds passing the overhead scene do not impart spectral noise, unlike a scanning spectrometer. Spectra are recorded by an indoor computer.

The amount of NO_2 is analysed by fitting differential laboratory cross-sections to the differential optical depths derived from the observed atmospheric spectra (Platt et al., 1979). Because scattered sunlight is used, the light path through the atmosphere will depend on the Solar Zenith Angle (SZA), and the measurements are of the slant column rather than the vertical column. Because there is no single path of scattered light, the effective slant path length through the atmosphere must be calculated via radiative transfer code. The ratio of this slant path length to the vertical is known as the Air Mass Factor (AMF), equal to about 2 at SZA 60° and about 18 at 90°, but AMF also depends on the wavelength, and on the vertical profiles of air density and NO_2.

The observed spectrum also contains Fraunhofer lines from the atmosphere of the sun, which would interfere with NO_2 absorption lines, but because these do not vary with SZA the observed spectra can be divided by a reference spectrum obtained at a small SZA to remove them. This reference spectrum also contains a small slant amount of NO_2 which by this division becomes subtracted from the actual slant amounts in the observed spectra.

However there can be significant errors in this method. The spectra are recorded by a solid-state detector with pixels, and because the temperature of the instrument is not controlled it expands and contracts moving the pixels along the spectrum. Due to this wavelength shift each recorded spectrum needs to be interpolated before it can be divided by the reference spectrum. Some interpolation methods cause the narrow Fraunhofer lines to be smoothed and so broadened, hence dividing these broadened lines by the narrower lines in the reference spectrum might create artefacts in the recorded spectra that can interfere with the measurement of the NO_2 absorption lines (Roscoe et al., 1996). Hence the amount of NO_2 in the reference spectrum might appear to change with the wavelength shift, being a minimum at shifts of 0 or 1 pixels and a maximum at shifts of -0.5 or 0.5. Any smoothing effect, and so artefact, is larger if there are fewer pixels within the slit width of the spectrometer.

3 Langley plots and their chemical modification

One way of treating the artefact due to wavelength shifts is via Langley plots. On a Langley plot the slant measurements of NO_2 are plotted against the associated AMFs to obtain a straight line, the gradient of which gives the vertical column and the intercept gives the negative of the actual amount of NO_2 in the reference spectrum plus the artefact (this sum is often called the effective amount in the reference spectrum). To get a useful Langley plot with a large range of AMF at least a half-day of data should be plotted.

Langley plots work well for trace gases which change only slowly during the day such as ozone, but the amount of NO_2 varies significantly during the day due to the interchange of NO_2 with NO and with reservoir gases such as N_2O_5. NO_2 reduces quickly at dawn when it is photolysed to NO, then increases quickly at dusk as NO falls almost to zero, while NO_2 also increases slowly during the day as N_2O_5 is photolysed and reduces slowly during the night as N_2O_5 is reformed (e.g. Roscoe et al., 1981).

Hence normal Langley plots cannot be used to accurately determine the vertical column of NO_2, instead we must use Langley plots with chemically modified AMFs, AMFs that have been multiplied by the ratio of the NO_2 vertical column at that time of day to the NO_2 vertical column at sunset (Lee et al., 1994), where the NO_2 is calculated by a model. In the chemically modified Langley plot all of the data points should now lie in a straight line. The intercept from the modified plot is then used with the slant measurements and unmodified AMFs to calculate the NO_2 vertical column at twilight (see below). This method allows Langley plots to be used to improve the accuracy of NO_2 vertical columns, and has been used to provide an improved analysis of NO_2 measurements between 1990 and 1995 at Faraday (Roscoe et al., 2001).

4 The chemical modification scheme and daily analysis

In order to use this method the variation in NO_2 during the course of the day needs to be known for different times of

the year. Hence an atmospheric photochemical box model is used to simulate it.

We use a variety of models and programs in the scheme, many of which are described by Denis et al. (2005). A photochemical box model is run as 24 stacked boxes to provide the profile through the atmosphere, and includes many different chemical species, gas phase reactions, photochemical reactions and heterogeneous chemical reactions (Chipperfield, 1999), with the amount of aerosol determined by the amount of H_2SO_4.

The box model was run for the climatological atmosphere over Faraday and then over Rothera, for 12 individual days in the year at about one month intervals to include both midwinter and midsummer (day numbers 21, 51, 81, 111, 141, 172, 202, 233, 264, 294, 325 and 355), each with a 10 day spin-up at constant day number. The climatology of air pressures, temperatures, and mixing ratios of different chemical species for the start of the runs were provided from a run of the Cambridge 2-D model, as used by some runs of the SLIMCAT atmospheric chemical transport model (Chipperfield, 1999), interpolated to the required latitude.

The radiative transfer model examines the different paths of scattered sunlight through the atmosphere to the spectrometer, using the profiles of NO_2 and ozone from the box model, to calculate the AMFs for NO_2 for a range of SZA during the course of each day. Aerosols are not included in this model. For each SZA the model considers multiple light paths through the atmosphere to the zenith sky spectrometer, which are either single scattered or double scattered, and adds up the transmitted light from each path after absorption by a given column of NO_2. The ratio of this result to the result with no NO_2 column then gives the AMF (Sarkissian et al., 1995).

At large SZA the scattered sunlight follows a long slant path through the atmosphere from the sun. Because of the curvature of the Earth, the SZA at each location along the path is less than the SZA directly above the spectrometer. By calculating the SZA at each location in the radiative transfer model, we can determine the mass-weighted mean SZA at each altitude, for use in the chemical box model. At a spectrometer SZA 89° the mass-weighted mean SZA over all altitudes is 88°.

Finally a program calculates the NO_2 vertical column at twilight (87° to 92° SZA), producing both dawn and dusk values for each day where measurements were obtained, by reading files containing one year of slant measurements, each with the day and time, SZA, detector temperature, wavelength shift, and the measurement error. It uses the NO_2 chemical ratios and AMFs from the models to produce modified Langley plots for each day.

Each AMF and chemical ratio (NO_2 vertical column relative to the sunset vertical column) used in the Langley plots is calculated by 2-D linear interpolation of the model results according to the SZA and the day number. On each plot a best-fit straight line with error is calculated by weighted least-squares fitting to obtain the intercept and error. A weighted mean of all these intercepts over the whole year of data is calculated. For each slant measurement around twilight an NO_2 vertical column is calculated using the mean intercept and the unmodified AMF (Eq. 1), and weighted mean vertical columns are calculated for both dawn and dusk on each day.

$$\text{Vertical\_column} = \frac{\text{Slant\_column} - \text{mean\_intercept}}{\text{AMF}} \quad (1)$$

NO_2 vertical columns at dawn and dusk were obtained for almost every day over the period 1990–2007, using in Eq. (1) the weighted mean of the modified Langley plot intercepts between 1 January and 31 December of the relevant year.

The resulting vertical columns at midsummer are examined in more detail by taking the weighted mean of the dawn and dusk columns from days 350–360 (16 to 26 December). One problem when assessing the midsummer trends is that the mean SZA of the twilight measurements varies, and the NO_2 vertical column changes rapidly with SZA at twilight. By using the box model simulation, the measured mean NO_2 vertical columns at dawn and dusk can be used to estimate the value at sunset (or 89° in the case of Rothera, where the sun never sets in midsummer), and the ratio of NO_y/NO_2 at sunset in the model can be used to estimate the NO_y vertical column.

It is tempting to use in Eq. (1) the individual intercepts to calculate the vertical columns for each day but for many days the error on the intercept is much too large to do this, particularly during winter. An alternative is to use estimates for the intercept calculated from the wavelength shift for each day. In principle this could be more accurate since the wavelength shift varies over the course of the year due to thermal expansion and contraction within the spectrometer, and we expect the intercepts of the modified Langley plots to reflect these variations. Using all the data the intercepts from the modified Langley plots were plotted against the wavelength shifts, the resulting relationship was used to provide daily intercepts from the wavelength shift, and the above calculations of midsummer NO_2 and NO_y repeated.

In the calculation of NO_y, partitioning of nitrogen species will depend on temperature, the amount of ozone (which affects both the amount of UV light and the gas phase chemistry) and the amount of aerosols, so we examined the sensitivity of NO_2 diurnal variations and NO_y/NO_2 ratios to these quantities.

Profiles of temperature and ozone were obtained from ECMWF, using ERA-40 until 2002, then ECMWF-Operational data, each at 1° resolution and 6-hourly intervals, courtesy BADC. The box model was run with these profiles for midsummer to provide more accurate NO_2 vertical columns, diurnal variations and NO_y/NO_2 ratios. The radiative transfer model was also re-run using the NO_2 and ozone profiles for each year to provide more accurate AMFs.

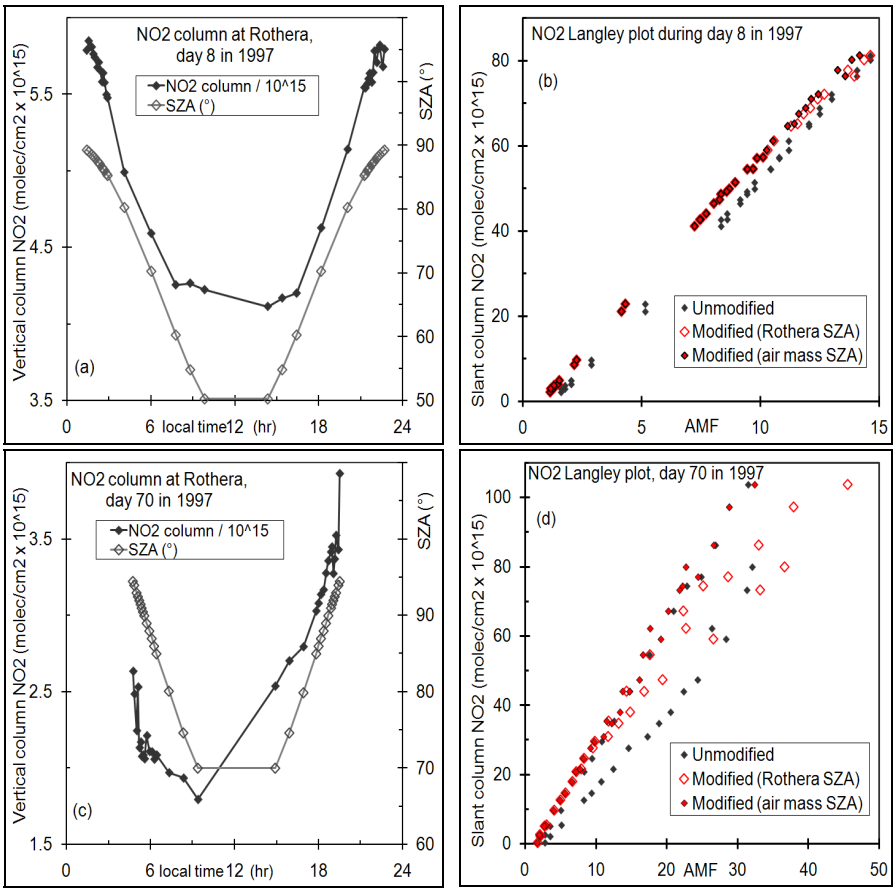

Fig. 1. Examples of the daily variation in NO_2 with time and SZA, and of the Langley plots produced for the analysis, for days 8 **(a–b)** and 70 **(c–d)** in 1997. Day 8 was in the summer when there was little N_2O_5, most of the variation was from the interchange between NO_2 and NO, and there is only a small difference between the morning and afternoon columns. However day 70 was in the autumn when most of the variation was from the interchange between N_2O_5 and NO_2, creating a large difference between the morning and afternoon columns. The Langley plots use unmodified Air Mass Factors (AMFs), AMFs modified by chemical ratios chosen from the Solar Zenith Angles (SZAs) at the spectrometer, and also AMFs modified by chemical ratios chosen from the mean SZAs for the air mass.

NO_2 vertical columns at dawn and dusk in midsummer were produced using both the observed profiles for each year and the climatology. Only the summer slant measurements were used in these studies, with midsummer mean intercepts (weighted mean of the modified Langley plot intercepts between 1 December and 15 January) and only AMF values and NO_2 chemical ratios from day 355 (21 December).

5 Results

Figure 1 shows examples of the daily variation in NO_2 and of the Langley plots produced for the analysis. Multiplying the AMFs by the NO_2 chemical ratios from the box model moves both the morning and evening values much closer to a single line, although this line curves down at large values of AMF when using SZAs at the spectrometer. Using the mean SZAs for the air mass makes the line straighter and the errors smaller.

The NO_2 vertical columns at twilight produced by the analysis are shown in Fig. 2. The difference between dawn and dusk is greatest during autumn and spring due to the large amounts of N_2O_5 at these times, and more variation in the NO_2 vertical columns is seen in spring when the site, near the edge of the polar vortex, alternately observes air from inside and outside the vortex. The midsummer and midwinter values vary from year to year, and the lower values of NO_2 in December 1991 and all of 1992 are due to the Mt. Pinatubo eruption in June 1991. The eruption greatly increased the amount of aerosols in the stratosphere over the following 18 months, leading to increased hydrolysis of both $BrONO_2$ and N_2O_5 to HNO_3, which titrates NO_2 to HNO_3. Note that the AMFs in 1991 and 1992 were not changed in this analysis (the error involved is less than 5%, Slusser et al., 1997).

The Langley plot intercepts are shown in Fig. 3. The intercepts have an annual cycle because the wavelength shift

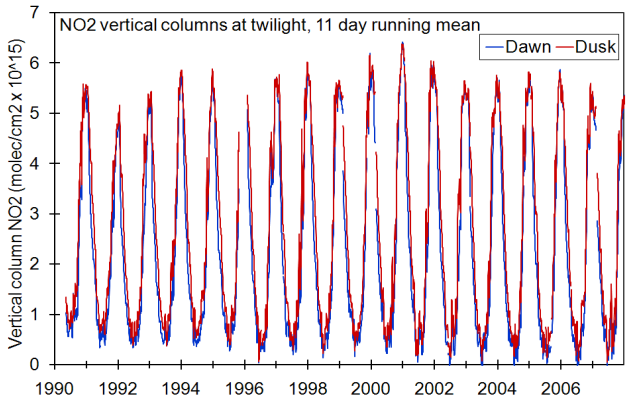

Fig. 2. The NO_2 vertical columns produced by the analysis at dawn and dusk twilight (87° to 92° SZA) with an 11 day running weighted mean, calculated using annual mean intercepts. The annual cycle of NO_2 with midwinter minima and midsummer maxima is clearly seen, and there is more NO_2 at dusk than at dawn. The spectrometer was moved from Faraday (65.25° S) to Rothera (67.57° S) in summer 1995 so no measurements were obtained during this period.

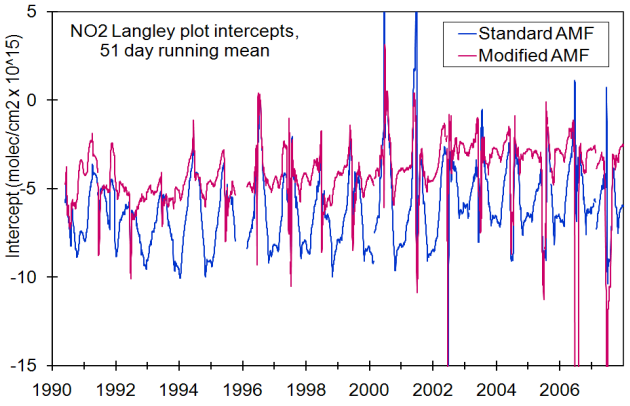

Fig. 3. The Langley plot intercepts produced by the analysis using unmodified and modified AMFs, with a 51 day running weighted mean. The modified AMFs produce much smaller intercepts, particularly at midsummer (note that the intercept equals the negative of the amount of NO_2 in the reference spectrum, plus any artefact). At midwinter the Langley plots are much poorer and give inaccurate intercept values because little of the NO_y is in the form of NO_2, and the range of SZA, and hence AMF, is small.

varies over the course of the year due to thermal expansion and contraction within the spectrometer. The modified AMFs produce smaller intercepts, particularly in summer, and are closer to the mean of the am and pm twilight amounts of NO_2 on the day of the reference spectrum, multiplied by the ratio of the AMF at the SZA of the actual reference spectrum to the mean twilight AMF (equal to 3.5×10^{15} molec/cm^2). The annual cycle is smaller since the artefacts are smaller and more constant with modified AMFs.

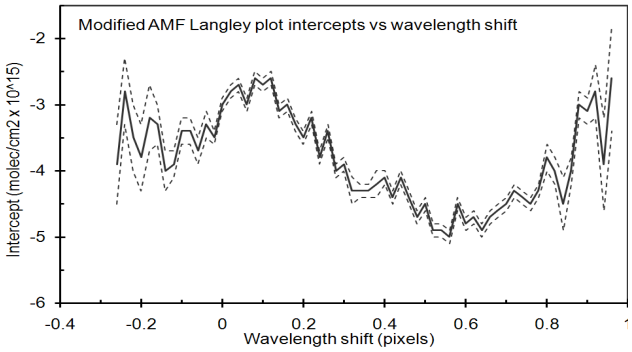

Fig. 4. The modified Langley plot intercepts versus the wavelength shift after binning, the solid line is the mean values and the dashed lines the standard deviations. We expect a repeating pattern with minima in the intercepts (small negative values) at shifts of 0 and 1 and maxima (large negative values) at shifts of −0.5 and 0.5. The pattern is actually displaced with a minimum around 0.1 and a maximum around 0.6, presumably due to a bias in the spectral analysis program.

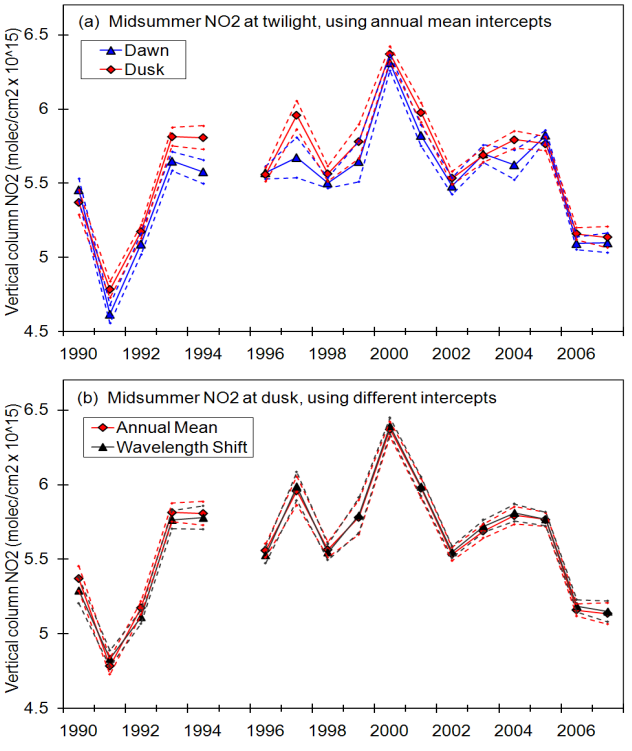

Fig. 5. The midsummer NO_2 vertical columns at twilight (87° to 92° SZA) for each year, weighted mean and standard deviation for the days 16 to 26 December. **(a)** Dawn and dusk columns calculated using annual weighted mean modified Langley plot intercepts, and **(b)** dusk columns calculated using annual mean intercepts, and daily intercepts estimated from the wavelength shift. There were no midsummer measurements in 1995.

Table 1. Trends in the NO_2 vertical column (%/decade) at midsummer sunset between 1990 and 2000 (excluding 1991 and 1992) and between 2000 and 2007, relative to values in 2000. The mean columns at dawn and dusk, calculated using either annual mean intercepts or wavelength shift intercepts, are interpolated to 89°. These trend fits are important for comparison with earlier work on trends in NO_2.

NO_2 trends from using annual mean intercepts		
	1990 to 2000	2000 to 2007
Dawn	9±4	−21±6
Dusk	11±4	−22±6
NO_2 trends from using wavelength shift intercepts		
	1990 to 2000	2000 to 2007
Dawn	11±4	−21±6
Dusk	13±4	−22±6

The modified Langley plot intercepts are plotted against the wavelength shift in Fig. 4. We expect a repeating pattern with smallest negative values at shifts of 0 and 1 and largest negative values at shifts of −0.5 and 0.5, but here they have been displaced to 0.1 and 0.6. The reason for this displacement is uncertain, but we speculate that it is related to the spectral analysis program searching for minimum residuals, always from negative to positive wavelength shift. To find the most probable relationship the plot was folded about 0.1 and 0.6 so that all the intercepts lay in the range 0.1 to 0.6, and a best-fit straight line with error was calculated by least-squares fitting.

We now look in detail at the analysed NO_2 vertical columns in midsummer, to consider any trends in NO_y. The midsummer values are the most useful for this because the NO_2 columns are largest here, and the N_2O_5 columns smallest so there is little sensitivity in the NO_y / NO_2 ratio to the amount of aerosols. Figure 5 shows the midsummer NO_2 vertical columns, using annual weighted mean intercepts of Fig. 3, and daily intercepts estimated from the wavelength shift in Fig. 4. Considerable year-to-year variation is seen and the values from 1991 and 1992 are low following the Mt. Pinatubo eruption. The midsummer reduction in 1991 (20%) and 1992 is almost entirely due to hydrolysis of $BrONO_2$ (Slusser et al., 1997), which is negligible for the amounts of aerosol observed between large volcanic eruptions. The pattern of trend and variability is almost identical using the two methods of analysis, with all differences smaller than the errors.

The typical error bar on a slant column of NO_2 at 88° SZA in summer is 3.6%. The typical error in vertical column on the mean of one twilight in summer is 1.4%, as expected from a mean derived from 7 to 9 slant-column measurements. The typical error in NO_2 vertical column from an 11-day mean in midsummer is 1%, as shown in Fig. 5 – larger than expected from the error in any one twilight because there is some variability in NO_2 during 11 days. The percentage errors in midsummer-mean NO_y are necessarily identical to those in NO_2.

To check that the year-to-year variations in Fig. 5 are not due to differences in the mean SZA of the measurements, thereby causing a different part of the daily variation to be observed, the midsummer columns were interpolated to 89° using the daily variation from the box model. The interpolated columns (not shown) coincide very well, the mean difference is only -0.01×10^{15} molec/cm^2, where the dusk and dawn columns have a mean difference of 0.09×10^{15} molec/cm^2. This coincidence gives support to the accuracy of the box model simulations. Much the same pattern of trend and variability to that in Fig. 5 is seen, with a broad maximum near 2000. This pattern could be construed as an upwards trend in the NO_2 vertical columns between 1990 and 2000 (excluding 1991 and 1992), and a downwards trend after 2000, in which case the gradients of the best-fit lines are given in Table 1. Using wavelength shift intercepts rather than annual mean intercepts again produces a very similar pattern and any differences in the possible trends (Table 1) are not significant.

Variations in the NO_2 vertical column do not necessarily follow variations in NO_y since the partitioning of nitrogen species depends on a number of factors, including temperature, ozone and aerosols. The box model was used to investigate the sensitivity of the midsummer NO_2 vertical column and NO_y/NO_2 ratio to these three factors.

Figure 6a shows the sensitivity of the model NO_2 vertical column to temperature. Increasing stratospheric temperature increases NO_2 while reducing the diurnal variation, but the sensitivity to realistic changes is modest at 0.5% K^{-1}.

Figure 6b shows the sensitivity to ozone. Changing the ozone column will change the amount of UV light reaching different levels of the atmosphere and will also affect the gas phase chemistry. Increasing the ozone reduces the NO_2 at the same altitude, due to the interaction quantified in Eq. (2) (Roscoe et al., 2001), but has little effect on the overall NO_2 column (0.05% for a 1% change in ozone) because of the compensating effect of reducing sunlight below, thereby increasing NO_2 below.

$$[NO]/[NO_2] = K_{(JNO2)} \exp(1200/T)/[O_3] \quad (2)$$

Figure 6c shows the sensitivity to aerosols, which is set in the box model by changing H_2SO_4. Increasing the aerosols slightly reduces the NO_2 column as more HNO_3 is produced, but the effect is small in midsummer at 0.28% for a 10% change in aerosol. Figure 6d shows the sensitivity of the NO_y/NO_2 ratio to temperature, and the ratio is seen to fall with increasing temperature. Using the temperature, ozone and aerosols in the climatology the box model gives a NO_y/NO_2 ratio of 3.8 at 89° SZA in midsummer, with the systematic errors listed in Table 2.

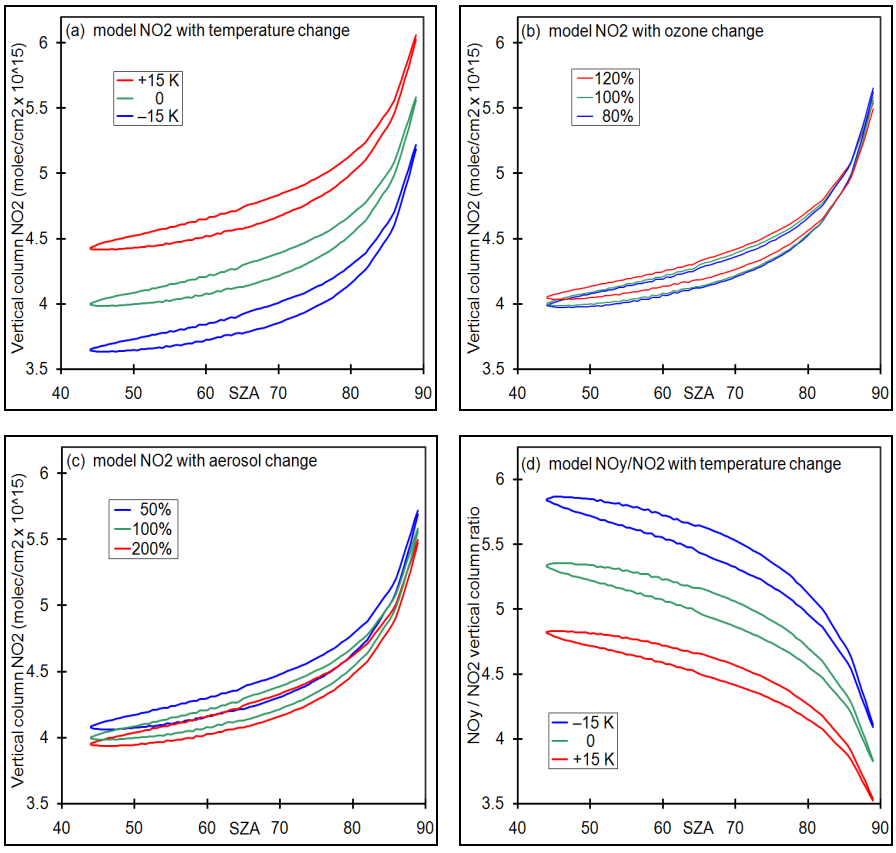

Fig. 6. The sensitivity of the box model NO_2 vertical column over Rothera in midsummer to temperature, ozone and aerosols, and the sensitivity of the NO_y/NO_2 ratio to temperature. Each shows the results from 3 simulations, with the unchanged climatology, and with the input values increased and reduced. **(a)** Stratospheric temperature increased and reduced by 15 K. **(b)** Ozone increased and reduced by 20% at all altitudes. **(c)** Aerosols doubled and halved at all altitudes (changes made to H_2SO_4 in the model). **(d)** The NO_y/NO_2 ratio in the 3 simulations at different stratospheric temperatures

Table 2. Sensitivities of NO_y/NO_2 to changes in temperature, ozone and aerosol used as input to the box model. The changes in each input represent probable errors in their observed decadal trends, so the values in the table represent systematic errors in the trend in NO_y for a given trend in measured NO_2. The right hand column then gives the estimated total systematic error in %/decade.

	temperature (/0.5 K)	ozone (/2 %)	aerosol (/20 %)	root-sum-square total
NO_y/NO_2	0.25 %	0.01 %	0.56 %	0.6 %

The partitioning of nitrogen species in the box model at midsummer is most sensitive to temperature with some sensitivity to ozone. Hence to better estimate trends in NO_2 and NO_y, actual rather than climatological temperature and ozone profiles are needed for each year at midsummer. ECMWF analyses provided temperature and ozone profiles over Faraday and Rothera. The box model was run with these profiles, and the radiative transfer model run with the resulting NO_2 and ozone profiles. The box model results for midsummer using the observed and climatological profiles are contrasted in Fig. 7. The NO_2 daily variations are very similar, though the vertical column is greater with the observed profiles by 0.8% on average and by 2.2% at twilight (87° to 89°).

Figure 8 shows the midsummer dawn and dusk columns interpolated to 89°, using the observed profiles and the climatology. The interpolated columns coincide well, the mean difference is again only -0.01×10^{15} molec/cm^2, and they again have much the same pattern of trend and variability as Fig. 5, with a broad maximum near 2000, and the differences

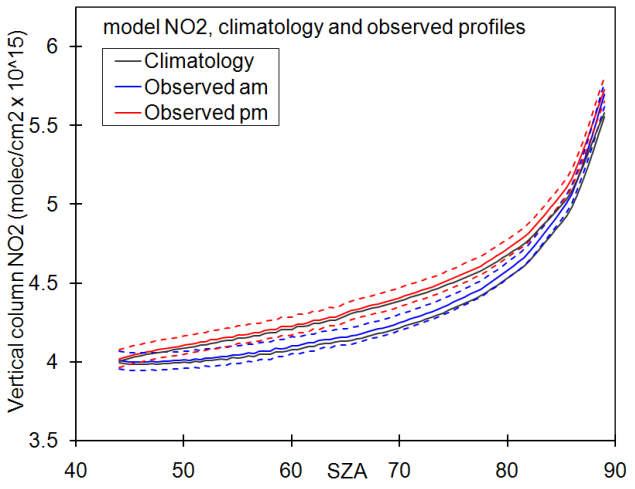

Fig. 7. The box model NO_2 vertical column over Rothera in midsummer, mean and standard deviation, using the observed temperature and ozone profiles (blue and red lines), and using the climatology (black line).

from using the climatology or observed profiles are minimal. Again, the pattern could also be construed as an upwards trend before 2000 followed by a downwards trend since, and the gradients of the best-fit lines are given in Table 3.

There is also potential for error in the trends because we used a single temperature for NO_2 cross sections during spectral analysis. The dependence of the slant columns of NO_2 on the temperature of the cross sections used, over our wavelength range, is 4% for 20 K, or 0.2%/K. The temperatures at 70 and 50 hPa in the ECMWF data that we used for NO_y calculation have standard deviations of 2.6 and 1.7 K, and trends of +0.6 and −0.6 K/decade, respectively. These translate to trends in NO_2 due to using a single temperature for cross-sections of +0.12%/decade and −0.12%/decade, small compared to total errors listed in Tables 2 and 3. The average trend from 100 hPa to 20 hPa is −0.14 K/decade, equivalent to 0.03%/decade, completely negligible.

Figure 9 shows the midsummer NO_y vertical columns using the observed profiles and the climatology. The NO_y columns are reduced when using the observed profiles, but otherwise the trends and variability are very similar. The gradients of the NO_y best-fit lines are given in Table 3.

Hence using observed profiles of temperature and ozone instead of the climatology makes little difference to the NO_2 values and the daily variation from the box model, but makes a significant difference to the NO_y values. However the patterns of trend and variability are almost identical irrespective of the method of analysis and irrespective of NO_2 or NO_y.

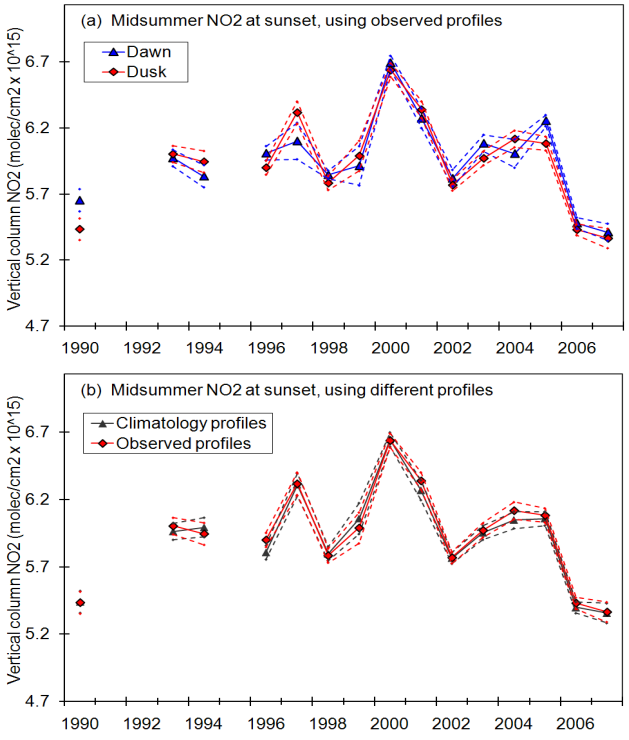

Fig. 8. The midsummer mean NO_2 vertical columns interpolated to 89° SZA (the maximum SZA at Rothera in midsummer, approximating to sunset). The values at twilight are interpolated according to the weighted mean SZA of the measurements, the diurnal variation of the NO_2 column in the box model for each year, and adjusted for the slightly larger NO_2 values in the climatology for the lower latitude at Faraday. **(a)** Interpolated dawn and dusk columns from using the observed profiles, and **(b)** interpolated dusk columns using the observed and climatology profiles. Values in 1991 and 1992 were excluded because of the effect in the box model of the greatly increased stratospheric aerosols from the Mt. Pinatubo eruption. In these calculations only the AMFs and NO_2 chemical ratios for day 355 were used, and the vertical columns were calculated using midsummer mean modified Langley plot intercepts (1 December to 15 January) rather than annual mean intercepts.

6 Interpretation and conclusion

The atmospheric photochemical box model, the radiative transfer model and the analysis routine form a useful method to analyse NO_2 slant measurements. By creating chemically modified Langley plots, more accurate vertical columns can be calculated, and by using the daily variation of NO_2 and the ratio of NO_y/NO_2 in the box model the vertical columns of NOy can be estimated.

The reduction in the NO_2 vertical columns in 1991 and 1992, due to increased hydrolysis of $BrONO_2$ and N_2O_5 on the aerosols from the Mt. Pinatubo eruption, are clearly seen (Slusser et al., 1997). These years are excluded from further discussion of trends and variability.

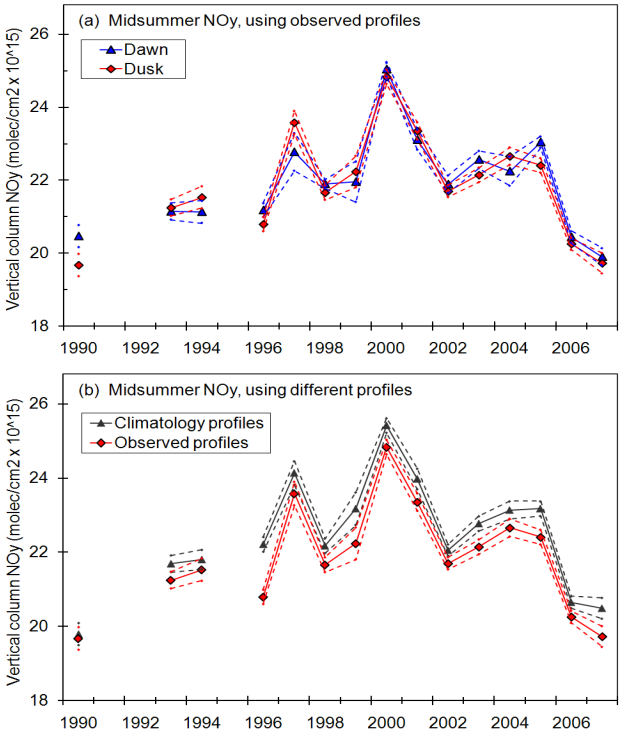

Fig. 9. The midsummer NO_y vertical columns, calculated from the NO_2 values at 89° SZA in Fig. 8 and the box model NO_y/NO_2 ratio at 89° for each year. **(a)** Interpolated dawn and dusk columns using the observed profiles, and **(b)** interpolated dusk columns using the observed and climatology profiles.

Table 3. Trends in the NO_2 and NO_y vertical columns (%/decade) at midsummer sunset between 1990 and 2000 (excluding 1991 and 1992) and between 2000 and 2007, relative to values in 2000. The mean NO_2 columns at dawn and dusk, using either climatology or observed profiles, are interpolated to 89°, then the NO_y columns are calculated from the NO_y/NO_2 ratio for each year.

NO_2 trends using box model results from climatology profiles		
	1990 to 2000	2000 to 2007
Dawn	10±4	−22±6
Dusk	12±5	−22±6
NO_2 trends using box model results from observed profiles		
	1990 to 2000	2000 to 2007
Dawn	9±4	−21±6
Dusk	11±5	−22±6
NO_y trends using box model results from climatology profiles		
	1990 to 2000	2000 to 2007
Dawn	15±4	−22±6
Dusk	17±4	−22±6
NO_y trends using box model results from observed profiles		
	1990 to 2000	2000 to 2007
Dawn	13±4	−22±6
Dusk	15±5	−23±5

The NO_2 vertical columns at midsummer produced by this method have only minimal changes when different intercept values are used, either weighted annual means or daily values from the wavelength shift. When interpolated to sunset, the dawn and dusk values coincide, giving confidence in the box model simulations. Once again the year-to-year pattern is almost unchanged. It is also almost unchanged when running the models with the observed profiles of temperature and ozone for each year instead of the climatology. All the analyses of NO_2 and NO_y columns at midsummer have a broad maximum near 2000, with significant inter-annual variability superimposed and little or no overall trend between 1990 and 2007 – simple fits of a trend line to NO_y between 1990 and 2007 result in a trend of 1±4%/decade. This is important because climate models that include a representative stratosphere and good resolution predict a significant increase in Brewer-Dobson circulation due to increased greenhouse gases (WMO, 2007; Butchart and Scaife, 2001). We explore overall trends with more rigour below.

The pattern could alternatively be construed as an increasing trend before 2000 and a decreasing trend since. Tables 1 and 2 list the fits to such trend lines, which range from 9 to 17%/decade before 2000 and −21 to −23%/decade after 2000. Earlier studies at 45° S have identified an increasing trend in NO_2 of about 5%/decade between 1980 and 1998 (Liley et al., 2000). If our measurements from 1990 to 2000 are taken as part of the same trend, our result is much larger at about 13%/decade. This suggests that a pair of opposing trends may not be a useful way of thinking about the observed pattern.

A better viewpoint could be that the changes in NO_y mostly consist of inter-annual variability, much of it at subdecadal scales but some with longer periods. From this viewpoint, the two sets of results could be consistent, because of the large NO_2 amounts observed in the early 1980s by Liley et al. (2000), plus our large maximum in NO_2 and NO_y in 2000. Other researchers studying the tropical lower stratosphere have also found implied changes in the Brewer-Dobson circulation and anomalies around 2000 that are correlated with atmospheric dynamics. Randel et al. (2006) calculated the mean tropical upwelling from the momentum balance in the atmosphere, finding that this decreased during the 1990s but has increased since 2000, and that both temperature and ozone above the tropical tropopause increased at many longitudes during 1999–2001 which are most probably due to changes in the mean tropical upwelling. Rosenlof

Table 4. Correlation slopes and t-values of multiple regressions, of mean dawn and dusk NO_2 at sunrise or sunset, and of mean dawn and dusk NO_y, against linear trend, QBO, solar-cycle and ENSO indices. Units of slopes of ENSO, QBO and solar flux are scaled so that 100 about equals the peak-to-peak amplitude of the index. From the double-sided Student t-test, a t-value of 1 is significant at 67%, and a t-value of 2 is significant at 95%.

	ENSO (%/4 K)	QBO (%/30 m s^{-1})	solar F10.7 (%/250 flux units)	Linear (%/decade)
NO_2 slope	8±6	−12± 6	15±9	−2.0±3.3
NO_2 t-value	1.3	2.0	1.8	0.6
NO_y slope	9±7	−11±6	20±9	1.1±3.5
NO_y t-value	1.4	1.7	2.2	0.3

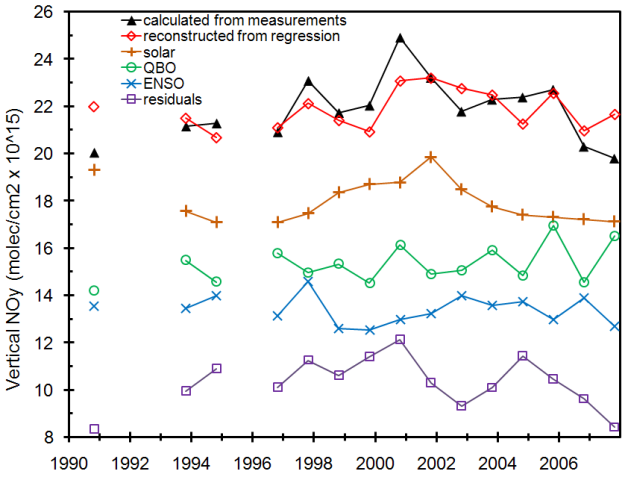

Fig. 10. Reconstruction from multiple regression of the mean midsummer NO_y at dawn and dusk (Fig. 9a), against solar cycle, QBO, ENSO and a linear component. The regression slopes are given in Table 4. The individual components due to solar cycle, QBO and ENSO are offset downwards, for clarity. The residuals are offset upwards. The linear component is not shown as its slope is negligibly small. The reconstruction explains 37% of the variance in the NO_y, including a similar proportion of the increase to 2000 and reduction since. There remains an unexplained cycle of amplitude at least 15% and of period at least 17 years.

and Reid (2008) found that the 1999–2001 warming of the tropical lower stratosphere was very pronounced and that this was strongly correlated with the QBO westerly phase.

Garcia-Herrera et al. (2006) found that the results from general circulation models implied that the El Nino Southern Oscillation (ENSO) signal propagates into the middle atmosphere by means of planetary scale Rossby waves, so that vertical wave propagation is enhanced during El Nino events but reduced during La Nina. Zeng and Pyle (2005) found that stratosphere/troposphere exchange increases during El Nino events, but decreases during La Nina. These two results suggest that the speed of the Brewer-Dobson circulation depends on ENSO, with a faster circulation during El Nino years.

To investigate the influence of ENSO and QBO on our results, plus the possible decadal influence of the solar cycle, we performed multiple regressions on the midsummer values of the mean of the dawn and dusk NO_2 at sunset/sunrise (Fig. 8a) and the similar mean of NO_y (Fig. 9a). We used the December (midsummer) monthly means of the following regression indices:

(a) for ENSO, the 3-month running mean of sea-surface temperature anomalies from 5° N to 5° S and 120 to 170° W (http://www.cpc.ncep.noaa.gov/products/analysis_monitoring/ensostuff/ensoyears.shtml)

(b) for QBO, the zonal wind over Singapore at 40 hPa (B. Naujokat, personal communication)

(c) for solar cycle, the radio-frequency F10.7 flux (ftp://ftp.ngdc.noaa.gov/STP/SOLAR_DATA)

(d) a linear term.

The results in Table 4 show that the solar cycle is well correlated and the QBO anti-correlated, each of them close to or above the 95% level. ENSO is less well correlated although it is still significant at the 90% level. The reconstruction components from the regression results for NO_y, shown in Fig. 10, shows that the maximum in NO_y in December 2000 is close to the solar maximum in 2001/2, and coincides with a strong negative QBO in December 2000. But although the regression accounts for 37% of the variance, much is unaccounted for. In particular, the residuals show that much of the increase up to 2000 and the reduction since is unexplained. This remains partially true even if the solar and QBO slopes are pushed to the limits of their error bars – the reconstructed value in 1990 then agrees, and the slope to 2000 almost disappears, but the slope since 2000 is almost doubled.

Importantly, the linear term from these regressions gives a much more rigorous trend estimate than a simple straight-line fit to the data. This is because dependence on slowly-varying quantities such as the solar cycle can impart a false trend that varies with start and end time of the data set. The results still show little or no overall trend, that in NO_y being

1.1±3.5%/decade. Including the total systematic error in Table 2 would increase this error bar by less than 0.1%/decade.

To investigate the relationship between trends in NO_y and trends in speed of the Brewer Dobson circulation, we constructed a simple multi-box model of the coupled troposphere and stratosphere (Cook and Roscoe, 2009). The results show that the trends are of opposite sign, and after subtracting the trend in tropospheric N_2O they are of almost equal magnitude (e.g. a 40% increase in speed results in a 39% decrease in NO_y). Tropospheric N_2O has been increasing by about 2.5%/decade (WMO 2007), so that our trend in NO_y signifies a small and not significant increase in Brewer-Dobson circulation of 1.4±3.5%/decade. The correlations with solar cycle and QBO in Table 4 imply equal correlations of opposite sign in Brewer-Dobson circulation: the speed of circulation follows the solar cycle with amplitude of about 20%, being slowest at solar maximum; and follows the QBO with amplitude of about 10%, being fastest at the positive phase of the QBO. There remains an unexplained cycle of amplitude at least 15% and of period at least 17 years, with a minimum in speed in about 2000.

Acknowledgements. Funding was provided by the EU as part of the GEOMON project (contract number 036677). ECMWF operational analyses data and ERA 40 reanalysis data were obtained from the British Atmospheric Data Centre. We thank the WinDOAS authors Michel van Roozendael and Caroline Fayt of IASB, Belgium, and Martyn P. Chipperfield and Wuhu Feng of the School of Earth and Environment, University of Leeds, UK, for the box model and the climatology. Finally, we thank referees for stimulating us to do the multiple regressions.

Edited by: A. Richter

References

Brewer, A. W.: Evidence for a world circulation provided by the measurements of helium and water vapour distribution in the stratosphere, Q. J. Roy. Meteor. Soc. 75, 351–363, 1949.

Butchart, N. and Scaife, A. A.: Removal of chlorofluorocarbons by increased mass exchange between the stratosphere and troposphere in a changing climate, Nature 410, 799–802, 2001.

Chipperfield, M. P.: Multiannual simulations with a three-dimensional chemical transport model, J. Geophys. Res., 104, 1781–1805, 1999.

Cook, P. A. and Roscoe, H. K.: Does an increase in the Brewer-Dobson circulation increase or reduce the amounts of stratospheric reactive gases?, submitted, Geophys. Res. Lett., 2009.

Denis, L., Roscoe, H. K., Chipperfield, M. P., Van Roozendael, M., and Goutail, F.: A new software suite for NO_2 vertical profile retrieval from ground-based zenith-sky spectrometers', J. Quant. Spectrosc. Ra., 92, 321–333, 2005.

Dobson, G. M. B.: Origin and distribution of polyatomic molecules in the atmosphere, Proc. R. Soc. Lond. A, 236, 187–193, 1956.

Garcia-Herrera, R., Calvo, N., Garcia, R. R., and Giorgetta, M. A.: Propagation of ENSO temperature signals into the middle atmosphere: A comparison of two general circulation models and ERA-40 reanalysis data, J. Geophys. Res., 111, D06101, doi:10.1029/2005JD006061, 2006.

Lee, A. M., Roscoe, H. K., Oldham, D. J., Squires, J. A. C., Sarkissian, A., Pommereau, J.-P., and Gardiner, B. G.: Improvements to the accuracy of measurements of NO_2 by zenith-sky visible spectrometers, J. Quant. Spectrosc. Ra., 52, 649–657, 1994.

Liley, J. B., Johnston, P. V., McKenzie, R. L., Thomas, A. J., and Boyd, I. S.: Stratospheric NO_2 variations from a long time series at Lauder, New Zealand, J. Geophys. Res., 105, 11633–11640, 2000.

McLinden, C. A., Olsen, S. C., Prather, M. J., and Liley, J. B.: "Understanding trends in stratospheric NO_y and NO_2", J. Geophys. Res. 106, 27787–27793, 2001.

Mount, G. H., Sanders, R. W., Schmeltekopf, A. L., and Solomon, S.: Visible spectroscopy at McMurdo station, Antarctica 1. Overview and daily variations of NO_2 and O_3, austral spring 1986, J. Geophys. Res., 92, 8320–8328, 1987.

Platt, U., Perner, D., and Patz, H. W.: Simultaneous measurements of atmospheric CH_2O, O_3 and NO_2 by differential optical absorption, J. Geophys. Res., 84, 6329–6335, 1979.

Pommereau, J.-P. and Goutail, F.: O_3 and NO_2 ground-based measurements by visible spectrometry during Arctic winter and spring 1988, Geophys. Res. Lett., 15, 8, 891–894, 1988a.

Pommereau, J.-P. and Goutail, F.: Stratospheric O_3 and NO_2 observations at the southern polar circle in summer and fall 1988, Geophys. Res. Lett., 15, 895–897, 1988b.

Randel, W. J., Wu, F., Vomel, H., Nedoluha, G. E., and Forster, P.: Deceases in stratospheric water vapor after 2001: Links to changes in the tropical tropopause and the Brewer-Dobson circulation, J. Geophys. Res., 111, D12312, doi:10.1029/2005JD006744, 2006.

Roscoe, H. K., Drummond, J. R., and Jarnot, R. F.: Infrared measurements of stratospheric composition. III. The daytime changes of NO and NO_2', Proc. R. Soc. Lond. A, 375, 507–528, 1981.

Roscoe, H. K., Fish, D. J., and Jones, R. L.: Interpolation errors in UV-visible spectroscopy for stratospheric sensing: implications for sensitivity, spectral resolution and spectral range, Appl. Optics, 35, 427–432, 1996.

Roscoe H. K., Charlton A. J., Fish D. J., and Hill J. G. T.: Improvements to the accuracy of measurements of NO_2 by zenith-sky visible spectrometers II: errors in zero using a more complete chemical model', J. Quant. Spectrosc. Ra., 68, 337–349, 2001.

Roscoe, H. K.: A review of stratospheric H_2O and NO_2, Adv. Space Res., 34, 1747–1754, 2004.

Rosenlof, K. H. and Reid, G. C.: Trends in the temperature and water vapor content of the tropical lower stratosphere: Sea surface connection, J. Geophys. Res., 113, D06107, doi:10.1029/2007JD009109, 2008.

Sarkissian A., Roscoe, H. K., and Fish, D. J.: Ozone measurements by zenith-sky spectrometers: an evaluation of errors in air-mass factors calculated by radiative transfer models, J. Quant. Spectrosc. Ra., 54, 3, 471–480, 1995.

Slusser, J. R., Fish, D. J., Strong, E. K., Jones, R. L., Roscoe, H. K., and Sarkissian, A.: Five years of NO_2 vertical column

measurements at Faraday (65° S): Evidence for the hydrolysis of $BrONO_2$ on Pinatubo aerosols', J. Geophys. Res., 102, 12987–12993, 1997.

WMO (World Meteorological Organisation), Scientific Assessment of Ozone Depletion: 2006, Global Ozone Research and Monitoring Project – Report No. 50, Geneva, 2007.

Zeng, G. and Pyle, J. A.: Influence of El Nino Southern Oscillation on stratosphere/troposphere exchange and the global tropospheric ozone budget, Geophys. Res. Lett., 32, L01814, doi:10.1029/2004GL021353, 2005.